Available online at www.sciencedirect.com
ScienceDirect
Journal of Solid State Chemistry 180 (2007) 2340–2345
JOURNAL OF SOLID STATE CHEMISTRY
www.elsevier.com/locate/jssc

Long Fe_3O_4 nanowires decorated by CdTe quantum dots: Synthesis and magnetic–optical properties

Xianmei Lan, Xuebo Cao*, Wenhu Qian, Weijian Gao, Cui Zhao, Yang Guo

Key Laboratory of Organic Synthesis of Jiangsu Province, Department of Chemistry, Suzhou University, Suzhou, Jiangsu 215123, PR China

Received 29 March 2007; received in revised form 30 May 2007; accepted 10 June 2007
Available online 16 June 2007

Abstract

This work describes the synthesis and magnetic–optical properties of Fe_3O_4 nanowires decorated by CdTe quantum dots. The composite nanowires with a length of 1 μm and an average diameter of 23 ± 3 nm were prepared in a high yield through the preferential growth of Fe_3O_4 on CdTe quantum dots using ethylenediamine as template. Their growth mechanism was discussed based on the results of control experiments. Studies on the optical and magnetic properties of the composite nanowires reveal that they assume not only yellow-green emission feature but also room temperature ferromagnetism.

Keywords: Bifunctional nanostructures; Magnetic; Photoluminescence; CdTe; Fe_3O_4

1. Introduction

After the great success in growing single-component nanocrystals with controlled dimensions and intriguing morphologies, researchers have paid attention to the fabrication of bifunctional nanostructures consisting of discrete domains of two materials [1–5]. Bifunctional nanostructures provide the possibility for enhanced functionality and multifunctional properties in contrast with their more-limited single-component counterparts [6–9]. One example of bifunctional nanostructures is magnetic–optical composite nanocrystal that combines magnetic nanoparticles and semiconductor quantum dots (QDs) [10–17]. This class of inorganic materials assumes not only magnetic properties but also photoluminescence properties, which can be applied in broad fields including bioassay, fluorescence detection, enhanced magnetic resonance imaging, selective magnetic separation, and information storage. For instance, Kim et al. [10] have reported the synthesis of Co/CdSe core–shell structure by the controlled deposition of CdSe onto preformed Co nanocrystals; Gu et al. [11] have shown a bifunctional heterodimer composed of quantum dot (CdS) and magnetic nanoparticle (FePt alloy) by taking advantage of lattice mismatching and selective annealing at a low temperature.

Most of the current reports in the field are focused on the deposition of semiconductor QDs onto spherical magnetic particles, while there are few reports on the combination of QDs with one-dimensional (1D) magnetic nanostructures (e.g., wires or rods) except for Ni nanowires functionalized with luminescent porphyrins [18], which is partly due to the difficulty in the preparation of 1D nanostructures of magnetic materials. Taking Fe_3O_4 for example, it does not grow preferentially by itself, mainly restricted by the isotropic spinel structure and the strong magnetism [19–23]. However, 1D magnetic–optical nanostructures are important due to their shape anisotropy, which can serve as very interesting building blocks for preparing unique superstructures that cannot be realized with spherical nanocrystals. In addition, due to the inter-face nano-confined effects, such types of the structures may be promising for the nonlinear optics and quantum electronics [24]. Recently, it has been demonstrated that inorganic nanoparticles can function as seeds to regulate the oriented growth of another crystal, and with this method, ZnO

*Corresponding author. Fax: +86 512 65880089.
E-mail address: xbcao@suda.edu.cn (X. Cao).

0022-4596/$ - see front matter © 2007 Elsevier Inc. All rights reserved.
doi:10.1016/j.jssc.2007.06.007

hexagons filled with Fe_3O_4 particles were obtained [25]. This study gives an important inspiration to grow 1D composite nanostructures.

In the present contribution, we use carboxyl-terminated CdTe QDs as seeds to modulate the preferential growth of cubic Fe_3O_4. In the presence of ethylenediamine, the co-precipitation of Fe^{3+} and Fe^{2+} on CdTe QDs produces long Fe_3O_4 nanowire decorated by CdTe QDs, which should be the first example of the combination of magnetic nanowires and luminescent semiconductor QDs. In the process of forming the composite nanowires, the highly anisotropic wurtzite structure of nonmagnetic CdTe helps to decrease the tendency of isotropic growth of cubic Fe_3O_4. Ethylenediamine, a strong alkaline coordinating agent, cannot only act as the mineralizer in the system but also join each other to form linear chains that provide the template for 1D growth of Fe_3O_4 [26–28].

2. Experimental

2.1. Synthesis of Fe_3O_4 nanowires decorated by CdTe quantum dots

To synthesize Fe_3O_4/CdTe composite nanowires, CdTe QDs stabilized by thioglycollic acid (TGA) were firstly prepared according to Zhang et al. [29]. Then, 10 mL degassed distilled water and 6 mL CdTe solution (0.01 mol/L) were added into a Teflon-lined stainless steel autoclave with a volume capacity of 30 mL. Four milliliters of benzene was laid on the water surface to isolate the system from atmosphere. Following that, stoichiometric $FeSO_4 \cdot 7H_2O$ (0.139 g) and $FeCl_3 \cdot 6H_2O$ (0.270 g) and 5 mL ethylenediamine were put into the liner, which would result in the formation of brown solution immediately. The autoclave was sealed and heated at 120 °C for 12 h. After cooling down to room temperature naturally, black solid was gathered from the liner. The black solid was selected carefully using a permanent magnet and washed with distilled water. In experiments, this process was repeated at least three times in order to remove uncombined CdTe QDs completely. The final product was dried in vacuum at 35 °C for 4 h for the subsequent characterization.

2.2. Characterization

X-ray powder diffraction (XRD) patterns were recorded on an X'Pert PRO SUPER rA rotation anode X-ray diffractometer with Ni-filtered Cu$K\alpha$ radiation ($\lambda = 1.54178$ Å). Transmission electron microscopy (TEM) images were taken with a FEI Tecnai G20 electron microscope, using an accelerating voltage of 160 kV. High-resolution transmission microscopy (HRTEM) images were taken at 200 kV with a JEOL-2010 TEM. Field-emitting scanning electron microscopy (FESEM) images were taken by a HITACHI S-4700 microscope operated at an accelerating voltage of 15 kV. Energy-dispersive X-ray (EDX) measurements were performed with the energy-

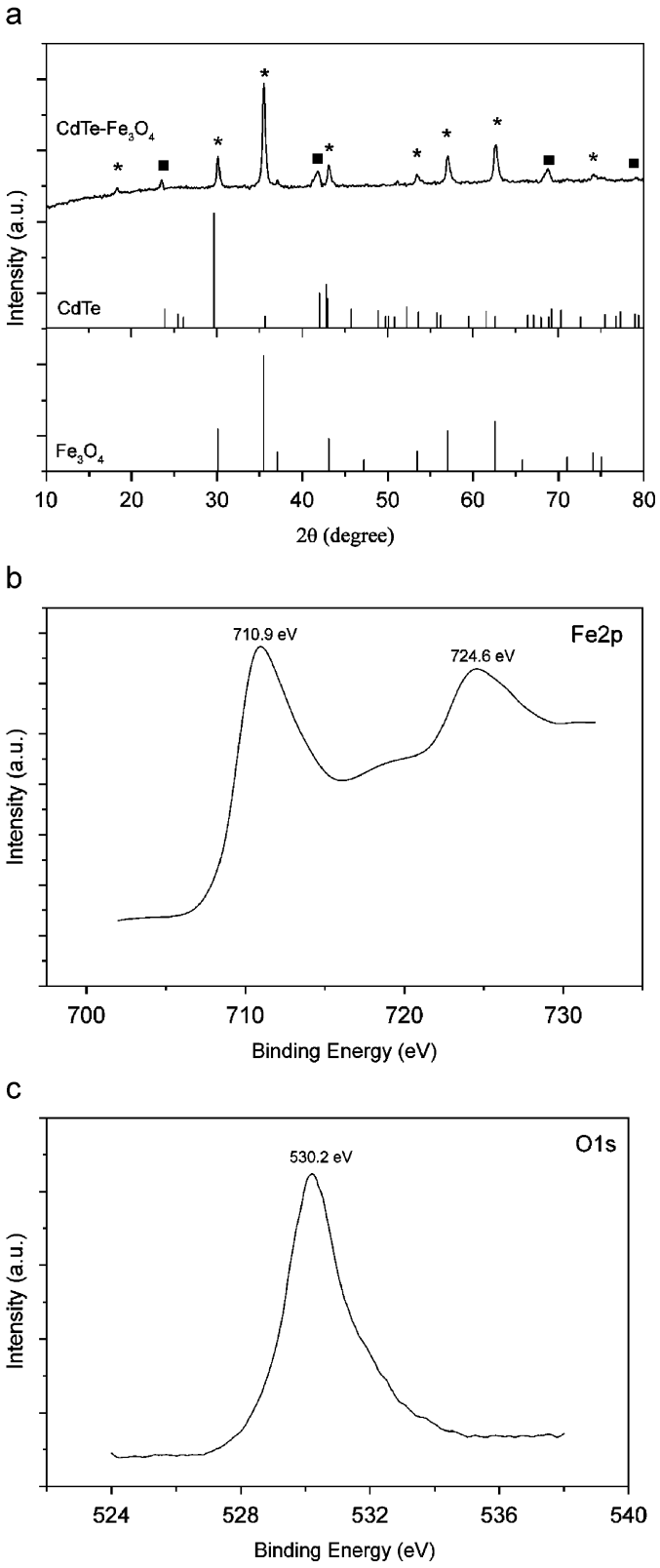

Fig. 1. (a) XRD pattern of Fe_3O_4 nanowires decorated by CdTe quantum dots, where the reflections marked by stars and squares correspond to magnetite and wurtzite CdTe, respectively. For comparison, standard patterns of Fe_3O_4 and CdTe are also included. (b) Binding energy spectrum for Fe 2*p*. (c) Binding energy spectrum for O1*s*.

dispersive X-ray spectrometer attached on the JEOL-2010 HRTEM. X-ray photoelectron spectra (XPS) were recorded on a VGESCALAB MK II X-ray photoelectron spectrometer using monochromatic Mg$K\alpha$ radiation ($hv = 1253.6$ eV) with a resolution of 1.0 eV. Optical absorption spectra were recorded on a Shimadzu 3150 UV–vis–near-infrared spectrophotometer. Photoluminescence spectra were performed on an Edinburgh FLS-920 Steady-State/Lifetime spectrofluorometer with Xe lamp as the excitation source. Hysteresis loops of the products were measured at room temperature by a BHV-55 vibrating sample magnetometer (VSM).

3. Results and discussion

Fig. 1a shows the typical XRD pattern of the Fe_3O_4/CdTe composite nanowires. The indexing of the reflections demonstrates that the major component in the product is cubic Fe_3O_4, together with minor wurtzite CdTe. Due to the closeness of the d value, parts of the reflections of wurtzite CdTe are overshadowed by the strong peaks of Fe_3O_4. Since carboxyl-terminated CdTe QDs are soluble in water and the product was washed repetitively with distilled water and selected using a permanent magnet, free CdTe QDs should be completely removed from the system. Therefore, CdTe detected in the product should be those attached to Fe_3O_4 tightly. In addition, since γ-Fe_2O_3 has an almost identical XRD diffraction pattern with Fe_3O_4, XPS was used to examine the Fe:O stoichiometry of the samples. Figs. 1b and 1c show XPS signals of the Fe 2p and O 1s regions. Two peaks of Fe 2p1/2 at 710.9 eV and Fe 2p3/2 at 724.6 eV were observed. The absence of the satellite peak situated at 719 eV, which is a major characteristic of Fe^{3+} in γ-Fe_2O_3, clearly excluded the formation of γ-Fe_2O_3 [30]. The O core level spectrum in Fig. 1c consisted of a mean peak originating from the oxygen in Fe_3O_4 (at 530.2 eV). The Fe/O ratio was estimated to be 0.76 with curve resolution analysis, which matches well with the stoichiometric ratio of Fe_3O_4 (0.75). Consequently, both the results of XRD and XPS demonstrate that Fe_3O_4/CdTe composites are synthesized.

Figs. 2a and b show the representative TEM image and FESEM image of Fe_3O_4/CdTe composites, respectively. As seen from the images, the dominant shape of Fe_3O_4/CdTe composites is the long nanowire. Additionally, there are also 5% spherical nanoparticles in the product. The length of the Fe_3O_4/CdTe composite nanowires is around 1 μm and their diameters are 23 ± 3 nm. Fig. 2c shows a HRTEM

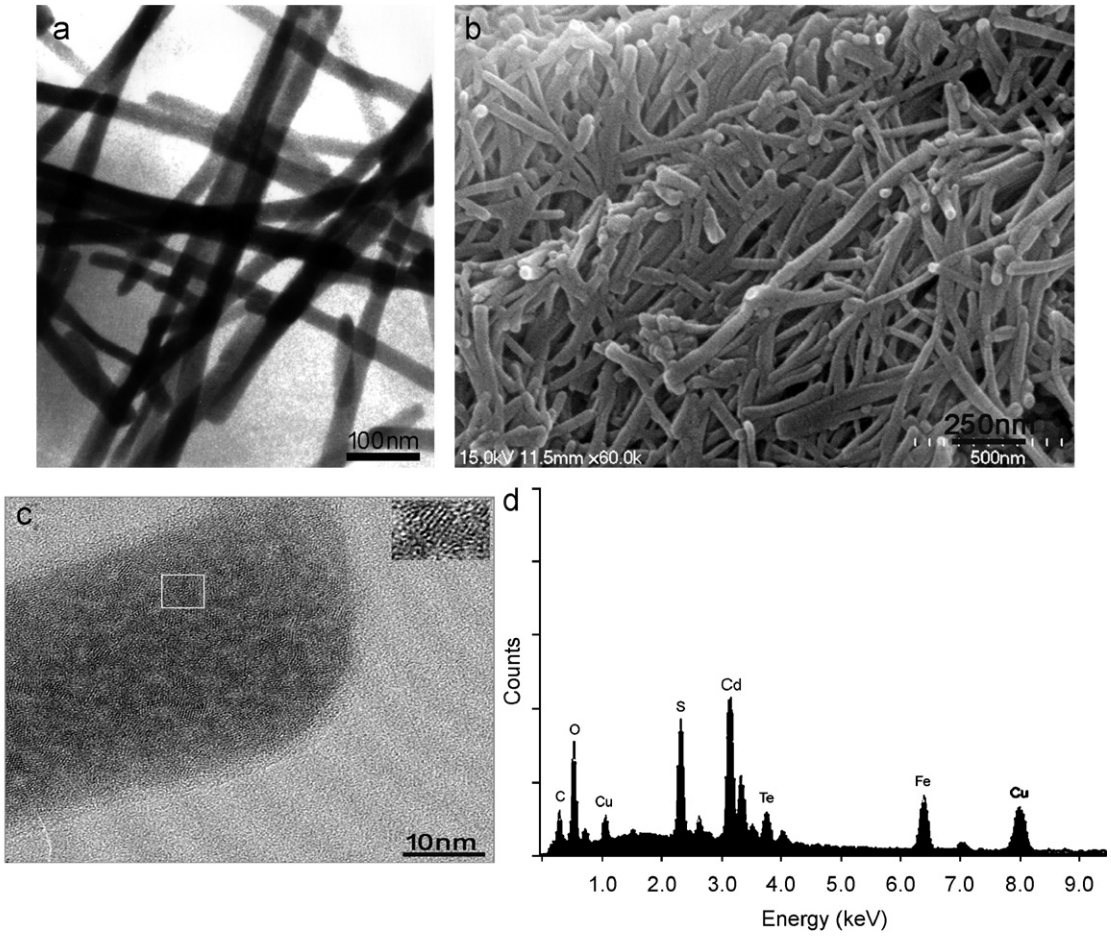

Fig. 2. (a) TEM image and (b) FESEM image of Fe_3O_4/CdTe composite nanowires. (c) HRTEM image of an individual nanowire, where the inset shows the magnified image of an individual crystallite embedded in the nanowire. (d) EDX spectrum recorded on the region marked by the box.

image of an individual nanowire; Fig. 2d is the associated EDX spectrum. From the HRTEM image, the domains between the nanowire and some small crystallites with size 4.6 nm are clearly seen, where the inset is the magnified image of one crystallite. The crystallites are presumed to be CdTe QDs because their size is very close to that of primary CdTe QDs. To confirm it, EDX spectroscopy is used to determine the exact components of them, which is performed by focusing the electron beam on the crystallite marked by the box. The elements associated with Fe_3O_4/CdTe such as Fe, O, Cd, and Te are all detected, but the major component of the crystallite is CdTe, as learned from its larger peak area. The S detected should link with TGA adsorbed on the surface of CdTe QDs. The signals of Cu and C originate from the carbon-coated copper grids onto which the sample is deposited. In a word, the studies of HRTEM and EDX demonstrate Fe_3O_4 nanowires decorated by CdTe QDs are successfully synthesized through the co-precipitation of Fe^{3+} and Fe^{2+} on CdTe QDs using ethylenediamine as mineralizer.

The growth mechanism of the composite nanowires is clarified through investigating the roles of ethylenediamine and CdTe QDs. If ethylenediamine was replaced by other alkaline mineralizers (e.g., $NH_3 \cdot H_2O$, NaOH) while keeping other conditions unchanged, the product would be irregular particle (Fig. 3a), same as those produced by conventional co-precipitation methods. If the reaction system did not contain CdTe QDs, the product would be straight and short nanorod rather than long wire (Fig. 3b). Consequently, it can be deduced that ethylenediamine in the system acts as the molecular template to direct the oriented growth of Fe_3O_4 while CdTe QDs can facilitate the formation of long wires, as described in Fig. 4. Ethylenediamine, a strong coordinating agent, can complex iron ions, and by means of hydrogen bonds, the complex ions would join each other to form linear chains that provide the template for the 1D growth of cubic Fe_3O_4 [26–28]. Although ethylenediamine can provide a linear template to direct the preferential growth of Fe_3O_4, its intrinsic isotropic structure and strong magnetism restrict it to develop into one-dimensional structure with a high aspect ratio. When CdTe QDs are introduced into the system, the high temperature and high pressure in the autoclave are advantageous to the attachment of them to Fe_3O_4 among the favorable crystallographic planes. The attachment of nonmagnetic CdTe to Fe_3O_4 will decrease the intrinsic strong magnetism of the latter and weaken the influences of it on the preferential growth of Fe_3O_4. And long Fe_3O_4/CdTe composite nanowires are formed eventually.

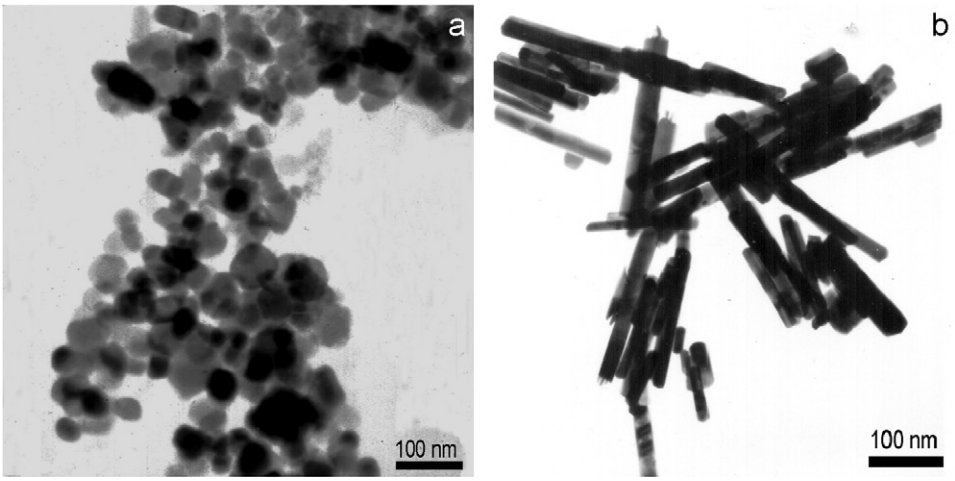

Fig. 3. (a) TEM image of the product prepared without ethylenediamine while keeping other conditions unchanged. The products are irregular particles. (b) TEM image of the product prepared without CdTe QDs while keeping other conditions unchanged. The products are short and straight nanorods.

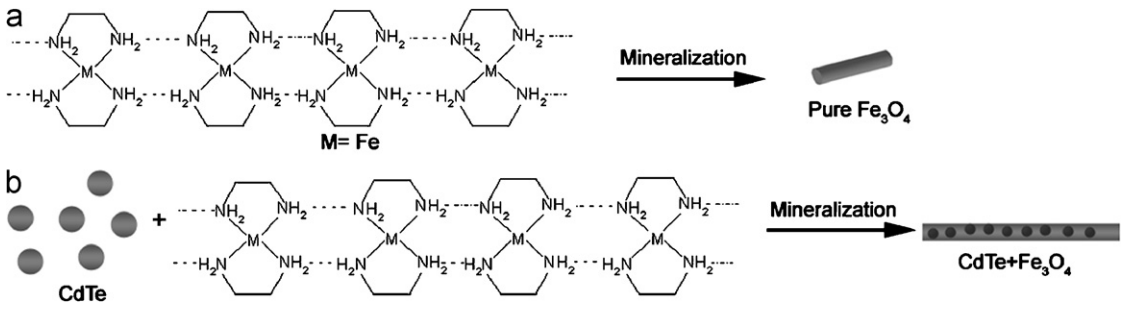

Fig. 4. Diagrammatical description of the growth mechanism of Fe_3O_4 nanorods and CdTe decorated Fe_3O_4 nanowires. For clarity, one ethylenediamine molecule is left out in the chelates.

Fig. 5 displays the room-temperature hysteresis loop of random Fe_3O_4/CdTe composite nanowires, which reveal that they exhibit a ferromagnetic behavior. The measured saturation magnetization of the nanowires is 52.4 emu/g, which is less than the values of nanoparticles or nanorods of pure Fe_3O_4 previously reported [19,22,26]. This result is related to the existence of nonmagnetic CdTe in nanowires. In addition, the shape anisotropy of nanowires would prevent them from magnetizing in directions other than along their easy magnetic axes, causing the decrease of the saturation magnetization [19,26,31].

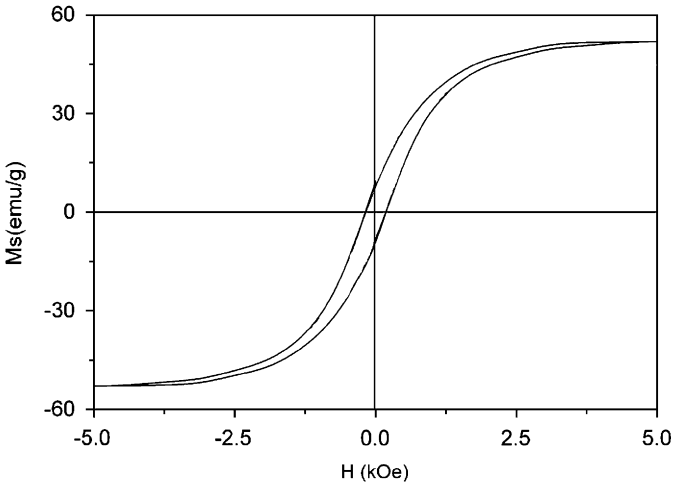

Fig. 5. Room-temperature magnetic loops of random Fe_3O_4/CdTe nanowires.

Absorption and emission spectra of Fe_3O_4/CdTe composite nanowires are presented in Fig. 6a. As a contrast, the absorption and emission spectra of primary CdTe QDs are also shown (Fig. 6b). For primary CdTe QDs, they exhibit narrow band-edge absorption around 560 nm and emission at 564.2 nm (Fig. 6b). For Fe_3O_4/CdTe composite nanowires (Fig. 6a), a broad absorption starting from near-infrared region is observed, which is characteristic of iron oxides [12,13]. However, the absorption due to CdTe is not apparent in the spectrum of Fe_3O_4/CdTe composite nanowires, which could arise from the overshadow of the absorption of CdTe QDs by the more prominent Fe_3O_4. But the luminescence effect of Fe_3O_4/CdTe composite nanowires is comparable to that of pure CdTe QDs except for a slight blue shift (1.7 nm) of the photoluminescence (PL) maximum. The blue shift can be attributed to the improved crystal quality of CdTe in the composite nanowires because they have suffered a thermal treatment in the autoclave. Upon illumination of a hand-held UV lamp, the Fe_3O_4/CdTe composite nanowires give off yellow-green emission (Fig. 6c), which further confirms that the properties of CdTe are preserved.

4. Conclusions

In summary, long Fe_3O_4 nanowires decorated by CdTe QDs are successfully prepared through the preferential growth of Fe_3O_4 on CdTe QDs as seeds. Ethyleneamine functions as mineralizer and template in the process of forming the composite nanowires. CdTe QDs can facilitate

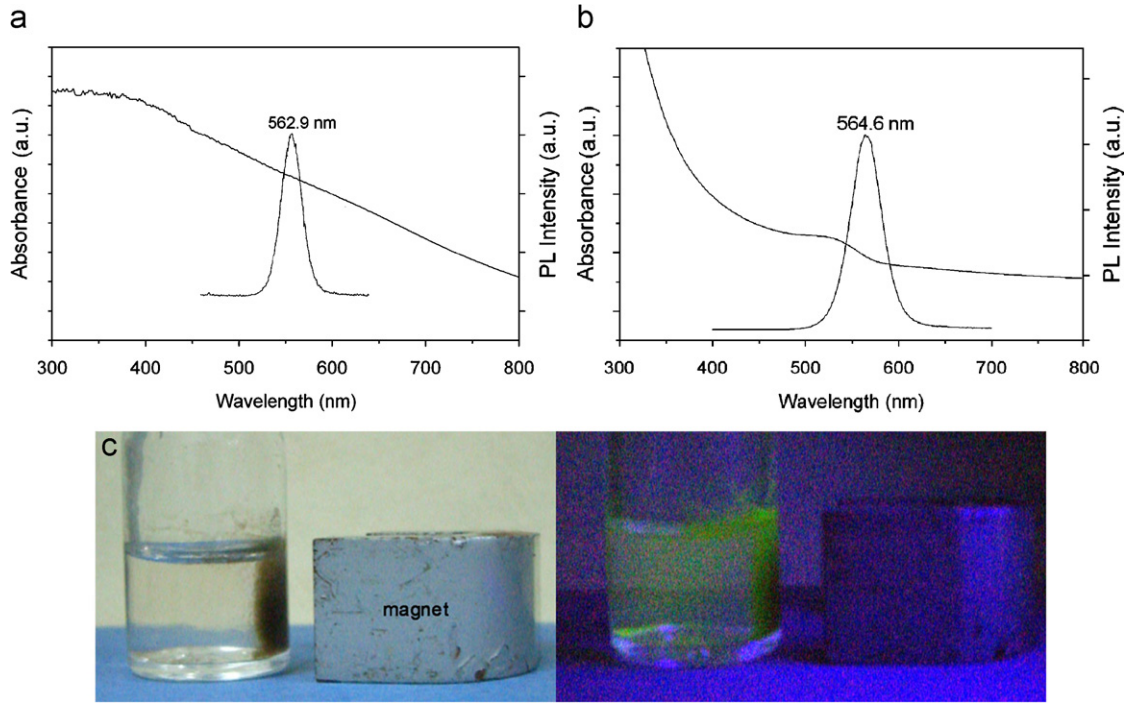

Fig. 6. Absorption and photoluminescence spectra of Fe_3O_4/CdTe composite nanowires (a) and primary CdTe QDs (b). The samples for spectra recording are prepared dispersing the nanowires into absolute alcohol. (c) Photography image of Fe_3O_4/CdTe composite nanowires dispersed in distilled water before and after UV excitation under an external magnetic field.

the tendency of anisotropic growth. The as-prepared nanostructure retains not only the good ferromagnetism of Fe_3O_4 but also the strong photoluminescence effect of CdTe QDs. The bifunctional Fe_3O_4/CdTe nanowires are expected to show applications in enhanced magnetic resonance imaging, selective magnetic separation, and the fabrication of nanoscale magneto-optics devices. Furthermore, investigations on their application are in progress.

Acknowledgment

This work was financially supported by the Key Laboratory of Organic Synthesis of Jiangsu Province (PR China) and National Natural Science Foundation of China (20601020).

References

[1] T. Mokari, E. Rothenberg, I. Popov, R. Costi, U. Banin, Science 304 (2004) 1787.
[2] Y. Li, Q. Zhang, A.V. Nurmikko, S. Sun, Nano Lett. 5 (2005) 1689.
[3] L. Li, J.C. Ren, J. Solid State Chem. 279 (2006) 1814.
[4] T. Pellegrino, A. Fiore, E. Carlino, C. Giannini, P.D. Cozzoli, G. Ciccarella, M.L. Respaud Palmirotta, R. Cingolani, L. Manna, J. Am. Chem. Soc. 128 (2006) 6690.
[5] J. Yang, H.I. Elim, Q.B. Zhang, J.Y. Lee, W. Ji, J. Am. Chem. Soc. 128 (2006) 6690.
[6] I. Robel, B.A. Bunker, P.V. Kamat, Adv. Mater. 17 (2005) 2458.
[7] T. Hirakawa, P.V. Kamat, J. Am. Chem. Soc. 127 (2005) 3928.
[8] H.Y. Lin, Y.F. Chen, J.G. Wu, D.I. Wang, C.C. Chen, Appl. Phys. Lett. 88 (2006) 161911.
[9] X.B. Cao, L. Gu, L.J. Zhuge, W.J. Gao, W.C. Wang, S.F. Wu, Adv. Funct. Mater. 16 (2006) 896.
[10] H. Kim, M. Achermann, L.P. Balet, J.A. Hollingsworth, V.I. Klimov, J. Am. Chem. Soc. 127 (2005) 544.
[11] H.W. Gu, R.K. Zheng, X.X. Zhang, B. Xu, J. Am. Chem. Soc. 126 (2004) 5664.
[12] L.J. An, Z.Q. Li, Z.J. Wang, H. Zhang, B. Yang, Chem. Lett. 3 (2005) 652.
[13] D.S. Wang, J.B. He, N. Rosenzweig, Z. Rosenzweig, Nano Lett. 4 (2004) 409.
[14] J. Kim, J.E. Lee, J. Lee, J.H. Yu, B.C. Kim, K. An, Y. Hwang, C.H. Shin, J.G. Park, J. Kim, T. Hyeon, J. Am. Chem. Soc. 128 (2006) 688.
[15] H.Y. Xie, C. Zuo, Y. Liu, Z.L. Zhang, D.W. Pang, X.L. Li, J.P. Gong, C. Dickinson, W. Zhou, Small 1 (2005) 506.
[16] G.P. Wang, E.Q. Song, H.Y. Xie, Z.L. Zhang, Z.Q. Tian, C. Zuo, D.W. Pang, D.C. Wu, Y.B. Shi, Chem. Commun. (2005) 4276.
[17] W.B. Tan, Y. Zhang, Adv. Mater. 17 (2005) 2375.
[18] M. Tanase, L.A. Bauer, A. Hultgren, D.M. Silevitch, L. Sun, D.H. Reich, P.C. Searson, G.J. Meyer, Nano Lett. 1 (2001) 155.
[19] J. Wang, Q.W. Chen, C. Zeng, B.Y. Hou, Adv. Mater. 16 (2004) 137.
[20] L. Feng, L. Jiang, Z.H. Mai, D.B. Zhu, J. Colloid Interface Sci. 278 (2004) 372.
[21] L. Shen, P.E. Laibinis, T.A. Hatton, Langmuir 15 (1999) 447.
[22] S.Y. Chen, J. Feng, X.F. Guo, J.M. Hong, W.P. Ding, Mater. Lett. 59 (2005) 985.
[23] D.H. Zhang, Z.Q. Liu, S. Han, C. Li, B. Lei, M.P. Stewart, J.M. Tour, C.W. Zhou, Nano Lett. 4 (2004) 2151.
[24] I.V. Kityk, in: T.B. Elliot (Ed.), Leading Edge Semiconductor Research, Nova Science Publishers, New York, 2005, pp. 1–61.
[25] R. Turgeman, S. Tirosh, A. Gedanken, Chem. Eur. J. 10 (2004) 1845.
[26] J.X. Wan, X.Y. Chen, Z.H. Wang, X.G. Yang, Y.T. Qian, J. Crystal Growth 276 (2005) 571.
[27] K. Soumitra, S. Chaudhuri, Chem. Phys. Lett. 398 (2004) 22.
[28] Y.D. Li, H.W. Liao, Y. Ding, Y.T. Qian, L. Yang, G.E. Zhou, Chem. Mater. 10 (1998) 2301.
[29] H. Zhang, L. Wang, H. Xiong, L. Hu, B. Yang, W. Li, Adv. Mater. 15 (2003) 1712.
[30] D.H. Zhang, Z.Q. Liu, S. Han, C. Li, B. Lei, M.P. Stewart, J.M. Tour, C.W. Zhou, Nano Lett. 4 (2004) 2151.
[31] Y.L. Chueh, M.W. Lai, J.Q. Liang, L.J. Chou, Z.L. Wang, Adv. Funct. Mater. 16 (2006) 2243.